High-performance yellow ceramic pigments $Zr(Ti_{1-x-y}Sn_{x-y}V_yM_y)O_4$ (M = Al, In, Y): crystal structure, colouring mechanism and technological properties

Michele Dondi, Francesco Matteucci, Isabella Zama

ISTEC-CNR, Institute of Science and Technology for Ceramics, Faenza, Italy

Giuseppe Cruciani

Department of Earth Sciences, University of Ferrara, Ferrara, Italy

Abstract

Zirconium titanate-stannate doped with V and Al, In or Y was synthesised by solid state reaction and its structural (XRD, SEM), optical (DRS) and technological properties were determined to assess its potential as ceramic pigment. These compounds have a srilankite-type, disordered orthorhombic structure, implying a random distribution of Zr, Ti, Sn and dopants in a single, strongly distorted octahedral site. Doping caused an increase of unit-cell dimensions, metal-oxygen distances and octahedron distortion. Optical spectra show crystal field electronic transitions of V^{4+} as well as intense bands in the blue-UV range due to V^{4+}–V^{5+} intervalence charge transfer and/or to V–O charge transfer. The formation of oxygen vacancies is supposed to compensate the occurrence of V^{4+} ensuring the lattice charge neutrality. These srilankite-type oxides develop a deep and brilliant yellow shade with colourimetric parameters close to those of industrial ceramic pigments. Technological tests in several ceramic applications proved that zirconium titanate-stannate is very stable at high temperature, exhibiting an excellent performance in the 1200-1250°C range, even better than praseodymium-doped zircon.

Key-words: A. ceramics, A. ceramic pigments, C. color, C. crystal structure, C. optical properties

1. Introduction

Ceramic prigments crystallizing with a srilankite-type structure (e.g. $ZrTiO_4$, space group Pbcn) were firstly developed in 1985 by Hund [1] who endeavoured to exploit the promising characteristics of zirconium titanate: i.e. very high refractive indices (2.33 < n < 2.41), high melting point (~1840°C), and the capacity to host a large variety of transition metal ions in its lattice.

Recently, the effect of Co, Cr, Fe, Mn, Ni, Pr, and V doping on the srilankite structure has been thoroughly re-examined together with colouring mechanisms and behaviour in ceramic applications [2]. Zirconium titanate pigments have a disordered structure, where both Zr and Ti are randomly distributed in a distorted octahedral site as well as chromophores and counterions added to impart colour. This $(Zr,Ti)O_2$ structure is able to develop a rather wide chromatic palette – ranging from green and greenish yellow (Co or Ni doping) to orange-buff (Cr or V doping) and brown-tan (Fe and Mn doping) – due essentially to a selective absorption of visible light connected with crystal field electronic transitions of chromophore ions. The lack of relevant charge transfer bands in the visible

spectrum let the colour be not pure and less saturated than that of current industrial ceramic pigments [2-5]. Furthermore, zirconium titanate exhibits an unsatisfactory technological performance, being to a considerable extent dissolved by chemically aggressive ceramic matrices, such as glazes for fast-fired tiles and tableware or liquid phase formed at high temperature in bodies for porcelain stoneware tiles. Therefore, the maximum temperature that zirconium titanate pigments can withstand without relevant colour changes is around 1000 °C [2].

In order to overcome these technological and colourimetric limits, Siggel and Jansen [6] designed a solid solution of zirconium titanate-stannate, that was doped with several combinations of a chromophore (i.e. a transition metal ion) and a counterion (i.e. an ion added to ensure the charge neutrality of the lattice). This solid solution is isostructural with srilankite and presents the same disordered cation distribution of zirconium titanate pigments [2,6-7]; nevertheless, it is able to develop more saturated colours. In particular, the co-doping with vanadium plus a trivalent counterion (i.e. Al, In or Y) gives rise to an intense and brilliant yellow coloration [6]. Despite the prospect of industrial application – consequent to a claimed thermal resistance up to 1200 °C – no detailed technological characterisation was carried out nor colouring mechanism was investigated to any extent.

The rationale of the present paper is assessing the colouring performance of the yellow pigments based on the $Zr(Ti_{1-x-y}Sn_{x-y}V_yM_y)O_4$ stoichiometry – where M stands for Al, In, or Y – in a wide range of ceramic applications, including frits and glazes for wall and floor tiles or sanitaryware as well as bodies for porcelain stoneware tiles. The colour of these zirconium titanate-stannates is compared with those of the most performant industrially-manufactured yellow pigments, i.e. praseodymium-doped zircon $(Zr,Pr)SiO_4$ [8], vanadium-doped baddeleyite $(Zr,V)O_2$ [9], and nickel-antimony-doped rutile $(Ti,Ni,Sb)O_2$ [3,10]. Furthermore, this paper is aimed at understanding which mechanism is responsible for the yellow coloration, by combining a detailed structural (XRPD) and spectroscopic characterisation (DRS).

2. Experimental

A set of three of samples, that in the text will be labelled with the symbol of doping ions, were prepared with the following stoichiometry: $ZrTi_{0.47}Sn_{0.47}A_{0.03}V_{0.03}O_3$, where A = Al, In, Y. The following oxides, with 99.9% of purity and particle size distribution of 20-30 μ m, were used as raw materials: Al_2O_3, In_2O_3, SnO_2, TiO_2, V_2O_5, Y_2O_3 and ZrO_2. No mineraliser was added. The powders were synthesised by the conventional ceramic process: wet mixing of raw materials in distilled water, drying in oven at 105°C overnight, pulverisation in agate mortar, then calcination in alumina crucibles in an electric kiln in static air at maximum temperature of 1400 °C, with thermal rate of 200°C/min, soaking time of 4 hours and natural cooling to room temperature. The calcined samples, previously dry ground in agate mortar and sieved below 50 μm, were characterised together with the industrial yellow pigments $(Zr,Pr)SiO_4$, $(Zr,V)O_2$ and $(Ti,Ni,Sb)O_2$, hereafter named ZP, ZV and RN respectively, by crystal structural, microstructural, spectroscopic and technological viewpoints.

X-ray powder diffraction was performed by a Philips PW1820/00 goniometer using graphite-monochromated Cu K$\alpha_{1,2}$ radiation, 15-130 °2θ measuring range, scan rate 0.02 °2θ, 10 s per step. The structural refinements were performed by the Rietveld method with the GSAS-EXPGUI software package [11,12]. Starting atomic parameters in the *Pbcn* space group for the disordered polymorph of zirconium titanate were taken from Siggel and Jansen [6] and used for all refinements. The independent refined variables ranged up to 26 including: scale-factors, zero-point, 15 coefficients of the shifted Chebyschev function to fit the background, zirconium titanate cell dimensions, atomic

positions, isotropic displacement parameters and profile coefficients: 1 gaussian (G_W) and 2 lorentzian terms (L_X, L_Y). The number of variables and observations as well as the figures-of-merit of all refinements are summarised in Table 1.

Microstructural analysis were carried out by Scanning Electron Microscopy (SEM, Cambridge Stereoscan 360, UK).

UV-visible-NIR spectroscopy was performed by diffuse reflectance with integrating sphere (Perkin Elmer λ 35, USA) in the 300-1100 nm range, step 0.3 nm illuminant D_{65} and observer 10°, using $BaSO_4$ as a reference. Reflectance measurements (R) were converted into absorbance data (A) by the Kubelka-Mink equation: $A = (1-R)^2 \cdot 2R^{-1}$ [16]. Optical spectra were deconvolved by gaussian bands for crystal field transitions and a lorentzian band for metal-oxygen charge transfer, using the software PFM (OriginLab).

Technological behaviour was assessed by adding the pigment into different ceramic matrices: a porcelain stoneware body (PS); two glazes for floor tiles: porcelain stoneware (S1) and stoneware (S2); a glaze (S3) and two frits (F1, F2) for wall tiles; a glaze for sanitaryware (S4). The pigment addition into the body (3% wt) was carried out by wet mixing, slip drying, powder deagglomeration in agate mortar, hand pelletisation (8% wt moisture), uniaxial pressing (40 MPa) of 25 mm-diameter disks, drying in oven (105°C) and firing in an electric roller kiln. Glazes and frits were added with 5% wt. pigment, wet mixed and the slip was sprinkled on porous ceramic tiles, then dried in oven and fired in an electric roller kiln. Ceramic coatings and porcelain stonware body were fast fired (60 min cold-to-cold) while the glaze for sanitaryware was fired with a slow cycle (24 hours cold-to-cold). The main chemical and physical characteristics of ceramic matrices are reported in Matteucci et al. [23]. The colour stability of pigments was evaluated by measuring the CIELab parameters by diffuse reflectance spectroscopy in the visible range (HunterLab Miniscan MSXP4000, 400-700 nm, white glazed tile reference x=31.5, y=33.3). Moreover, different pigment loadings (1, 2, 3, 4 and 5% wt) were added to the frit F1, in order to draw curves of colour saturation versus colorant percentage; thus actual concentration of the colouring phase was taken into account for industrial pigments, that contain also a filler (Table 1).

3. Results and discussion

3.1. Crystal structure

Zirconium titanate-stannate pigments were synthesized in rounded to sub-euhedral prismatic ~~crystals~~crystallites, mostly ranging from 2 to 8 μm in size and in between 1.0 and 1.8 of aspect ratio (Fig. 1).

These compounds have the same srilankite-type disordered structure of the undoped $ZrTi_{0.5}Sn_{0.5}O_4$, implying a random distribution of Zr, Ti, Sn and dopants in a unique octahedral site (Fig. 2). It is so confirmed the role of tin and dopants in the low temperature stabilisation of the ~~the~~ high temperature disordered phase [2,6-7].

The addition of vanadium plus ~~aluminum~~aluminium, indium or yttrium provoked some significant changes in the crystallographic parameters with respect to the $ZrTi_{0.5}Sn_{0.5}O_4$. In fact, a noticeable increase of the unit-cell volume occurred, connected with a strong growth of the dimension *a*, a limited increase of the parameter *c* and nearly steady values for *b* (Tab. 1). Only displacements of the oxygens from their atomic positions are basically involved: a trend YV < InV < AlV is appreciable for x(O) and z(O), but viceversa for y (Tab. 2). These structural variations are not proportional with the difference of the averaged cationic radius <R> between $ZrTi_{0.5}Sn_{0.5}O_4$ (<R> 68.4 pm) and the samples doped with Al and V (<R> 68.0 pm), In and V (<R> 68.4 pm), or Y and V (<R> 68.6 pm); these latter have a larger unit-cell not simply explainable with an increase of the mean size of the ions occupying the octahedral site. ~~An increased electrostatic repulsion of cations/anions~~

A change in the ordering state of the octahedral cations, undetectable in the refined average structure, might be an explanation for this anomalous behaviour [2].

Structural differences have also repercussions on the metal-oxygen and metal-metal distances as well as on the degree of distortion of the cationic site (Tab. 2). In the undoped zirconium titanate stannate, the octahedral site is tetragonally distorted, in particular vertically compressed, the apical distance M-$O_{3,4}$ (2.05 Å) being shorter than the equatorial M-$O_{1,2}$ and M-$O_{5,6}$ ones (on average 2.07 Å). Doping had a distinct effect on the AlV pigment on the one side and on InV or YV on the other side. The former exhibits a pronounced shortening of the apical bonding M-$O_{3,4}$ (2.02 Å) and an elongation of both equatorial distances (on average 2.09 Å). The latter pigments show increased apical distance (2.07 Å) and further distortion of the octahedron equatorial plane, with shorter M-$O_{1,2}$ and longer M-$O_{5,6}$ bonds with respect to the undoped lattice. Thus, the octahedron varies from vertically compressed (AlV) to slightly vertically elongated (YV) with the sample InV having almost equivalent mean apical and equatorial distances. Correspondingly, a clearly increased quadratic elongation Δ_6 occurred with doping, as values grew from 1.34 (undoped zirconium titanate stannate) up to 1.92 (YV); InV has the less distorted octahedron (Δ_6=1.79) among pigments. On the other hand, doping caused just little changes of metal-metal distances, being the M_1-$M_{4,5,6,7}$ only slightly increased and the M_1-$M_{2,3}$ practically unaffected (Tab. 2).

3.2. Optical properties

Srilankite-type ceramic pigments develop an intense and vivid yellow colour, showing significant differences upon the co-doping with Al, In or Y (Tab. 4). In particular, the sample InV exhibits a purity of colour close to that of Pr-doped zircon (ZP) that is the brightest yellow pigment on the ceramic market; however, InV is somewhat less brilliant (i.e. lower L*), less yellow (slightly lower b*) and has a weak red cast, not present in ZP. The sample AlV is characterised by colourimetric parameters less intense than ZP, but substantially analogous to those of V-doped baddeleyite (ZV), and free of the slight red component shown by InV. The sample YV is brighter than AlV or InV and has an intermediate b* value, though it exhibits a little green cast; these characteristics resemble those of nickel-antimony-doped rutile (RN).

The optical spectra present two clearly distinct features (Fig. 3): weak absorption peaks in the infrared-visible range and a strong band at the edge of the ultraviolet region, which – absorbing practically all the violet wavelengths – causes the perception of a yellow colour by human eye [13]. These spectra were successfully deconvolved by two gaussian bands at lower energy, corresponding to crystal field (CF) electronic absorptions, plus two further bands (one gaussian and one lorentzian) at higher energy, probably referable to metal-oxygen charge transfer (MLCT).

The two CF transitions occur as rather broad bands (FWHM = 3000-3800 cm^{-1}) at $\sim$ 12,300 cm^{-1} (ν_1) and $\sim$ 15,500 cm^{-1} (ν_2) with a decreasing intensity from AlV to YV (Tab. 4). The ν_1/ν_2 ratio is gradually reduced in the same direction: AlV (1.35), InV (0.62), YV (0.38). These transitions can be assigned to V^{4+}, as no light absorption is expected below $\sim$ 16,000 cm^{-1} for V^{3+} and below $\sim$ 22,000 cm^{-1} for V^{5+} [14-16]. At all events, a single absorbance band is described for intermediate valence oxides, with wavenumber increasing from $\sim$ 14,900 cm^{-1} (V_7O_{13}) to $\sim$ 15,900 cm^{-1} (V_3O_5); i.e. from prevailing V^{4+} to prevalently V^{3+} [17].

The electronic configuration of V^{4+} implies a single CF transition $^2T_{2g}(^2D) \rightarrow ^2E_g(^2D)$ in octahedral coordination, that however is often split in three energy levels, owing to a dynamic Jahn-Teller effect occurring in low point symmetry sites, such as that of the

srilankite structure [14-16]. On this basis, the transition ν_1 can be attributed to $^2A_g \rightarrow$ $^2B_{1g}, ^2B_{2g}$, as ν_2 can be assigned to $^2A_g \rightarrow ^2B_{3g}$ (Fig. 4). These weak absorptions are responsible for the small chroma differences among srilankite-type pigments: the stronger intensity of both peaks in AlV, for instance, justifies the lack of any red cast, while the decreasing ν_1/ν_2 ratio accounts for the red and green contribution of InV and YV respectively.

The high energy part of the spectrum is constituted by two intense and very broad bands (FWHM = 3900-8500 cm^{-1}) ranging from the near UV (ν_4 = 26,000-28,000 cm^{-1}) to the blue-violet region (ν_3 = 22,900-24,100 cm^{-1}). The former can be surely referred to a MLCT, even if such Ti^{4+}–O^{2-} (and perhaps Zr^{4+}–O^{2-}) transition occurs at $\sim$ 30,000 cm^{-1} in the undoped ZrTiO$_4$ [2]. The latter band is the main responsible of the yellow coloration of zirconium titanate-stannate and its origin seems to be mainly related with the $^2A_g \rightarrow ^2A_g$ transition of V^{4+}, though it is too intense for a parity-forbidden crystal field peak. Hence, an important contribution can be due to a V^{4+}–O$^-$ charge transfer and/or to a V^{4+}–V^{5+} intervalence charge transfer; both phenomena give rise to an absorption band at 24,800-26,000 cm^{-1} [18-19]. However, a further contribution by a V^{5+}–O^{2-} charge transfer, manifesting in V^{5+}-bearing glasses as a very sharp absorption band at ~25,000 cm^{-1}, cannot be excluded [16,18]. Interestingly, the most pure yellow colour corresponds to the steeper slope of the ν_3 band, achieved with the V and In co-doping.

3.3. Crystal structural vs optical properties

The crystal field transitions of V^{4+} ion inside the octahedral site of zirconium titanate-stannate are compared with those in several oxides differing for coordination, size and distortion of the cationic site (Tab. 5). The energy of the three transitions $^2A_g \rightarrow ^2B_{1g}, ^2B_{2g}$, $^2A_g \rightarrow ^2B_{3g}$ and $^2A_g \rightarrow ^2A_g$ is very close to that shown by V^{4+} in the zirconium silicate, despite the considerable differences in metal-oxygen distances and site geometry, and besides spectroscopic terms in cubic coordination are inverted with respect to the octahedral one.

The crystal field strength of the V^{4+} ion in octahedral environment may be estimated assuming a symmetric splitting of the t$_{2g}$ and e$_g$ terms (Fig. 4):

$$\Delta_o = {}^2E_g - {}^2T_{2g} = ({}^2A_g + {}^2B_{3g})/2 - ({}^2B_{1g}/2).$$

However, the first term is somewhat affected by probable interference by charge transfer effects on the excited state ^2A_g, while the second term is neglecting the actual energy of the ground state ^2A_g, that cannot be determined by optical spectroscopy. The Δ_o values calculated for zirconium titanate-stannates and V^{4+}-bearing oxides (Table 4), including industrial ceramic pigments, appear to be actually correlated with the inverse fifth power of the mean metal-oxygen distance, somewhat fitting the principles of crystal field theory [14,16] though this relationship is not satisfactory for SnO$_2$ (Fig. 5).

Although the srilankite-type pigments are following this general trend, their mutual Δ_o differences do not correspond to their relative changes in metal-oxygen distances: quantitative measurements of optical spectra are too uncertain to allow a strict correlation with so small variations in V-O distances.

A certain role may be played by the thermodynamical stability of the V^{4+} ion in octahedral coordination: in fact, its crystal field stabilization energy (CFSE) is larger in vertically compressed sites (CFSE = $^2/_5 \Delta_o + ^2/_3 \delta$, where δ is the $^2A_g \rightarrow ^2B_{1g}, ^2B_{2g}$ splitting) than in vertically elongated ones (CFSE = $^2/_5 \Delta_o + ^1/_3 \delta$) [14]. Being both Δ_o and δ of the same order of magnitude (i.e. ~13000 and ~12000 cm^{-1} respectively) the CFSE is significantly larger in AlV (about -160 kJ/g·ion) than in YV (around -110 kJ/g·ion) with InV having an intermediate value due to its almost equivalent apical and equatorial metal-oxygen distances. Therefore, V^{4+} in zirconium titanate-stannate is expected to be more stable in the decreasing order: AlV > InV > YV.

The remarkable intensity of the ν_3 band could be due to a contribution by a $V^{4+}\rightarrow V^{5+}$ intervalence charge transfer [18-19] whose energy is believed to depend on the distance between the two vanadium ions in adjacent sites of the lattice [14]. Once the mean metal-metal distances of several V-bearing oxides is contrasted with the ν_3 position in their spectra, the expected positive correlation is appreciable (Fig. 6) the only outlier neing zircon, where V^{4+} should occur in both cubic and tetrahedral coordination [24].

The occurrence of V^{4+}, perhaps predominant over V^{5+}, implies an intriguing deviation from the designed stoichiometry of the srilankite-type pigments, where any Ti^{4+} + Sn^{4+} substitution was thought by a V^{5+} + M^{3+} (M=Al, In or Y) pair [6]. It is improbable that any charge deficiency due to V^{4+} instead of V^{5+} could be compensated by either Zr^{4+}, Ti^{4+}, Sn^{4+} or Al^{3+}, In^{3+}, Y^{3+}, that are all ions very reluctant to any further oxidation. Thus, the most convincing mechanism appears to be an oxygen vacancy, so that the actual stoichiometry, e.g. of pigment InV, is probably very close to:

$$Zr\ Ti_{0.47}\ Sn_{0.47}\ V^{4+}_{0.03}\ In_{0.03}\ O_{3.985}.$$
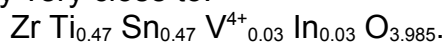
Interesting enough, the colouring mechanism of zirconium titanate-stannate is somehow analogous to those of the other yellow ceramic pigments, as these latter all exhibit a sharp absorbance band at the blue-violet border, that is due to:

– vanadium-doping of zirconia (ZV), probably a phenomenon similar to that acting in the srilankite-type pigments, attributed to V–O charge transfer and/or V^{4+}–V^{5+} IVCT [9].
– Praseodymium-doping of zircon (ZP), as far as it is known, causing a metal-oxygen charge transfer Pr^{4+}–$O^{2-} \rightarrow Pr^{3+}$–$O^{-}$ [10,25,26].
– Nickel doping in rutile (RN) is responsible for several weak peaks in the red-orange region (CF electronic absorptions of Ni^{2+}) and a strong band due to the $^3A_2(^3F) \rightarrow ^3T_1(^3P)$ transition of Ni^{2+} coalesced with the Ti^{4+}–O^{2-} charge transfer [3,10].

3.4. Technological performance

The technological behaviour of both srilankite-type and industrial ceramic pigments was appraised from different points of view: a) colouring performance in several ceramic applications, i.e. the absolute value of yellow shade (b* parameter); b) thermal and chemical stability, in contact with liquid phases differing greatly for composition and firing temperature, expressed as the change of yellow colour in the ceramic ware (b^*_c) in respect of the untreated pigment (b^*_p), i.e. the b^*_c/b^*_p ratio; c) capacity of colour saturation, calculated as the intensity of yellow weighed for the pigment concentration in the same ceramic matrix.

Colouring performance opf industrial pigments is characterised by a quite regular decrease of b* values with firing temperature for ZP and RN, but a rather steady coloration of ZV (Fig. 5A). ZP ensures the most yellow shade at all temperatures; RN performs satisfactorily at lower temperature, decreasing fastlyrapidly its b* value over 1050°C, so that ZV gives better results for the highest thermal levels. The zirconium titanatea-stannate pigments exhibit a different trend versus temperature, with a good colouring performance below 1100°C, being intermediate between ZP and ZV, a rapid drop of b* to the worst values in between 1100 and 1150°C, then excellent development of yellow shade for temperatures $\geq$ 1200°C (Fig. 5A). Very interestingly, the sample InV performs even better than ZP in the 1200-1250°C range, that at present is the most important for large scale applications (e.g. porcelain stoneware tiles); also AlV and YV present b* values very close to zircon and zirconia pigments in such a thermal interval.

Once data are expressed in terms of colour stability, it is possible to appreciate that all pigments behave similarly at the lower temperatures, but exhibit a distinct performance at intermediate and high thermal levels (Fig. 5B). In particular, the srilankite-type pigments present a very good stability in the 1200-1250°C range, being better than ZP and practically the same of ZV; conversely, they are quite easily attacked by ceramic glazes

fired in the 1100-1150°C range, where they are much less stable than any industrial pigment. This behaviour is clearly connected with the completely different chemical environment of ceramic glazes and bodies used at high temperatures (e.g. porcelain stoneware and sanitaryware) or intermediate temperatures (e.g. fast-fired wall and floor tiles). Very interestingly, the ranking of chemico-physical stability at high temperatures – as appreciable from Figure 5B (i.e. AlV > InV > YV) – corresponds to the order of decreasing thermodynamical stability of the chromophore ion V^{4+} in the srilankite lattice. A statistical approach, performed by principal components analysis, allows a qualitative interpretation of the relationships among colour stability of srilankite-type pigments and chemical composition of ceramic matrices (Fig. 6). It can be seen that CaO is the most critical component, as falling at the opposite side of the ellipse, it is negatively correlated with the stability of AlV, InV and YV pigments, so resulting the main responsible for the chemical attack at intermediate temperatures. PbO and B_2O_3 seem to play a stabilizing role, being close to the pigments' points on the ellipse, that is only apparent, because these components are essentially present in low temperature glazes and glassy coatings, where zirconium titanate-stannate is highly stable. At any event, it is interesting that some of the most aggressive oxides in the glazes – i.e. BaO, MgO and especially ZnO – appear to have just negligible effects on the srilankite-type pigments.

The capacity to ensure a high colour saturation was assessed contrasting the parameter b* versus the actual concentration of ceramic pigment in a glassy coating (Fig. 7). Zirconium titanate-stannate has more or less the same capacity than the industrially-manufactured RN and ZV, though ZP has still an unrivalled yellow saturation.

4. Conclusions

A $ZrTiO_4$-$ZrSnO_4$ solid solution containing V and Al, In or Y was synthesised by solid state reaction, resulting in a brilliant and saturated yellow coloration, even at a low doping level (0.03 mol.%). These compounds have a srilankite-type crystal structure with a disordered cation distribution in a single octahedral site, where Zr, Ti, Sn and dopants are randomly ~~accomodated~~accommodated. Dopants provoked an increasing of the unit-cell dimensions, metal-oxygen distances and octahedron distortion with respect to undoped $Zr(Ti,Sn)O_4$, that are not proportional to the change of mean cationic size induced by V and Al, In or Y. This suggest that the involved substitution mechanism to achieve charge balance might not be simply ascribed to the heterovalent isomorphous replacement. Moreover, variations in the ordering state of the octahedral cations, undetected in the refined average structure, cannot be ruled out to explain the unit cell ~~The structural variations~~ changes~~could be due to …….~~.

Optical spectra are characterised by a strong absorption band at the violet-UV edge, responsible for the deep yellow shade, assigned to V^{4+}–O^- charge transfer and/or to a V^{4+}–V^{5+} intervalence charge transfer. Minor chroma variations are due to crystal field electronic transitions of V^{4+} in the NIR-orange region. The occurrence of V^{4+} implies a positive charge deficiency in respect of the designed pair substitution $Ti^{4+} + Sn^{4+} \rightarrow V^{5+} + M^{3+}$ (M=Al, In or Y) that is probably balanced by oxygen vacancies.

Srilankite-type pigments exhibit colourimetric features to a large extent analogue to those of the most ~~performant~~perform ant yellow pigments on the ceramic market. Their colouring performance is excellent at high temperature – particularly in glazes and bodies for porcelain stoneware tiles that are usually fired in the 1200-1250°C range – being even better than Pr-doped zircon and V-doped zirconia, i.e. the best industrially-manufactured yellow ceramic pigments. Zirconium titanate-stannate is suitable also for low temperature application (i.e. 900-1050°C) in alkali-borosilicate glassy coatings, even if containing PbO. At all events, these pigments cannot be utilised for wall tiles, typically fired in the

1100-1150°C range, because easily dissolved by the abundant CaO present in these glazes.

References

[1] F. Hund, Z. Anor. Allg. Chem. 525 (1985) 221-229.
[2] M. Dondi, F. Matteucci, G. Cruciani, J. Solid State Chem. (2006) in print.
[3] F. Matteucci, G. Cruciani, M. Dondi, M. Raimondo, Ceram. Int. (2005) in print.
[4] R.A. Eppler, Am. Ceram. Soc. Bull. 66 (1987) 1600-1604.
[5] P. Escribano LÚpez, J.B. Carda CastellÚ, C.E. Cordoncillo, Esmaltes y pigmentos cer‡micos, Faenza Editrice Iberica, p. 300, 2001.
[6] A. Siggel, M. Jansen, Z. Anor. Allg. Chem. 58 (1990) 93-102.
[7] A.E. McHale, R.S. Roth, J. Am. Ceram. Soc. 69 (1986) 827-32.
[8] J.A. Badenes, J.B. Vicent, M. Llusar, M.A. Tena, G. MonrÛs, J. Mater. Sci. 37 (2002) 1413-1420.
[9] F. Ren, S. Ishida, N. Takeuchi, J. Am. Ceram. Soc. 76 (1993) 1825-1831.
[10] S. SorlÌ, M.A. Tena, Badenes J.A., Calbo J., M. Llusar, G. MonrÛs, J. Eur. Ceram. Soc. 24 (2004) 2425-2432.
[11] A.C. Larson, R.B. Von Dreele, Los Alamos National Laboratory Report LAUR. (2000) 86-748.
[12] H. Toby, J. Appl. Cryst. 34 (2001) 210-213.
[13] K. Nassau, The Physics and Chemistry of Color, Wiley & Sons, New York, 2001, p. 481.
[14] R.G. Burns, Mineralogical applications of crystal field theory, Cambridge University Press, 2nd edition, 1993.
[15] A.B.P. Lever, Inorganic electronic spectroscopy, Amsterdam, Elsevier, 2nd edition, 1984.
[16] S. Marfunin, Physics of Minerals and Inorganic Materials, Springer-Verlag Berlin Heidelberg New York,1979.
[17] V.R. Porter, W.B. White, R. Roy, J. Solid State Chem. 4 (1972) 250-254.
[18] J. Cao, J. Choi, J.L. Musfeldt, S. Lutta, M.S. Whittingham, Chem. Mater. 16 (2004) 731.
[19] L.J. Burcham, G. Deo, X. Gao, I.E. Wachs, Topics in Catalysis 11-12 (2000) 85.
[20] Y. Yonesaki, K. Tanaka, J. Si, K. Hirao, J. Phys.: Condens. Matter 14 (2002) 13493.
[21] Y. Kera, Y. Matsukaze, J. Phys. Chem. 90(1986) 5752.
[22] C. Kikuchi, I. Chen, W.H. From, P.B. Dorain, J. Chem. Phys. 42 (1965) 181.
[23] F. Matteucci, C. Lepri Neto, M. Dondi, G. Cruciani, G. Baldi, A.O. Boschi, Adv. Applied Ceram. 105 (2006) in print.
[24] M. OcaÒa, A.R. Gonzalez-Elipe, V.M. Orera, P. Tartaj, C.J. Serna, J. Am. Ceram. Soc. 81 (1998) 395-400.
[25] M. OcaÒa, A. Caballero, A.R. Gonz·lez-Elipe, P. Tartaj, C.J. Serna, J. Solid State Chem. 139 (1998) 412-415.
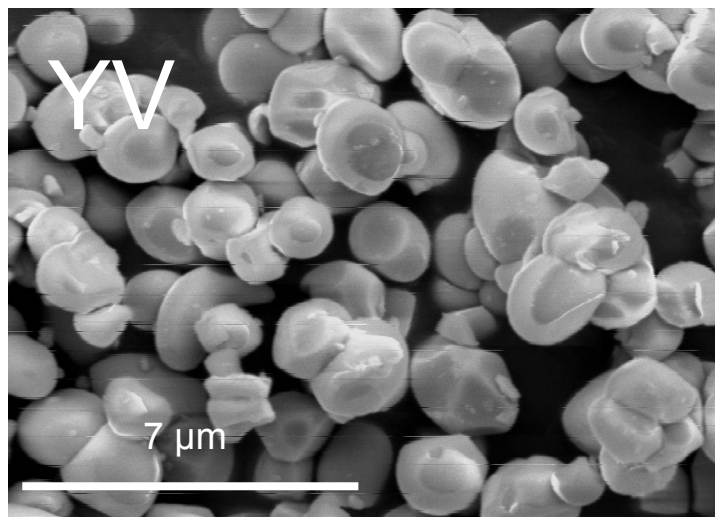[26] G. Del Nero, G. Cappelletti, S. Ardizzone, P. Fermo, S. Gilardoni, J. Eur. Ceram. Soc. 24 (2004) 3603-3611.
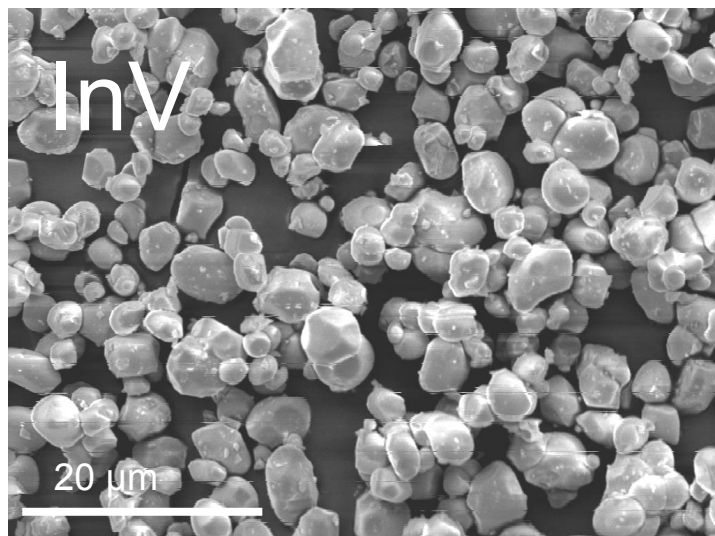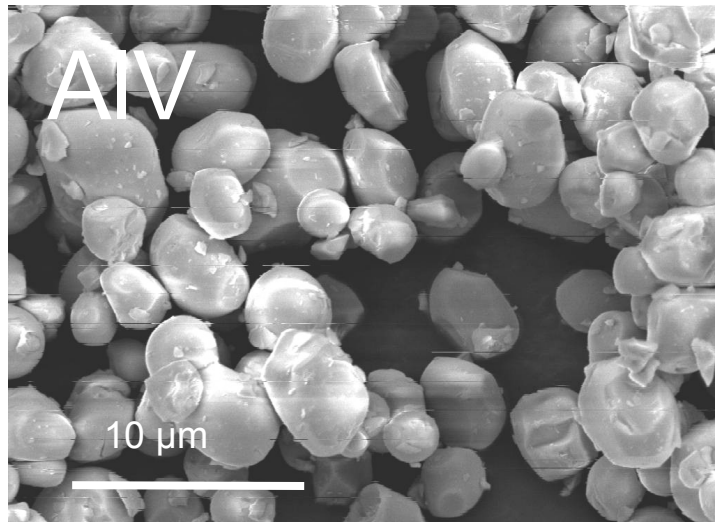
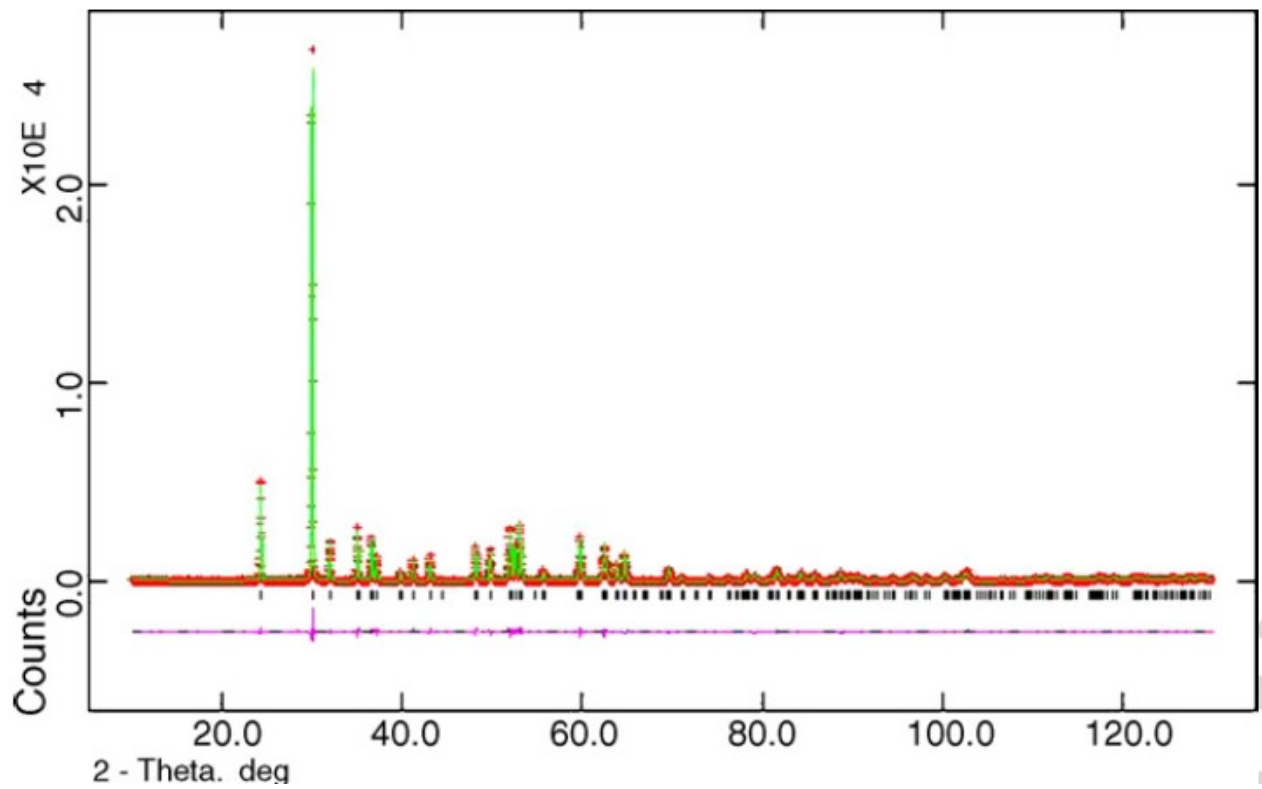Fig. 1. SEM photomicrographs of srilankite-type ceramic pigments.

Fig. 2. Rietveld refinement plot of the X-ray powder diffraction data of the sample InV. In the figure the continuous line represent the calculated pattern, while cross points show the observed pattern. The difference curve between observed and calculated profiles is plotted below.
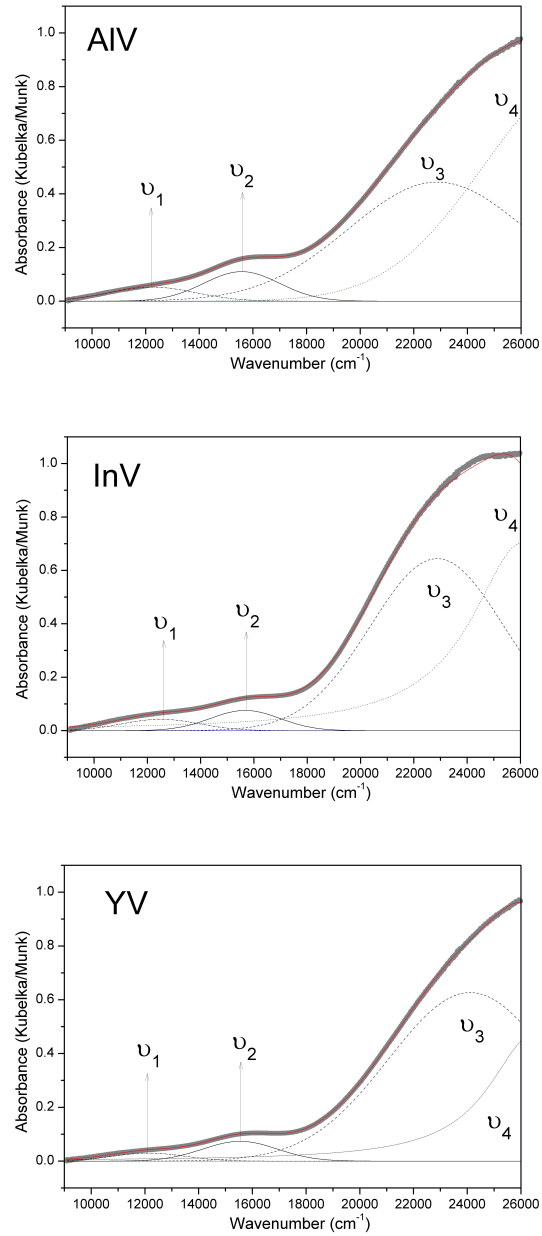
Fig. 3. Diffuse reflectance spectroscopy of the srilankite-type pigments. Spectra are deconvolved in three gaussian bands (υ_1, υ_2 and υ_3) and one lorentzian band (υ_4).
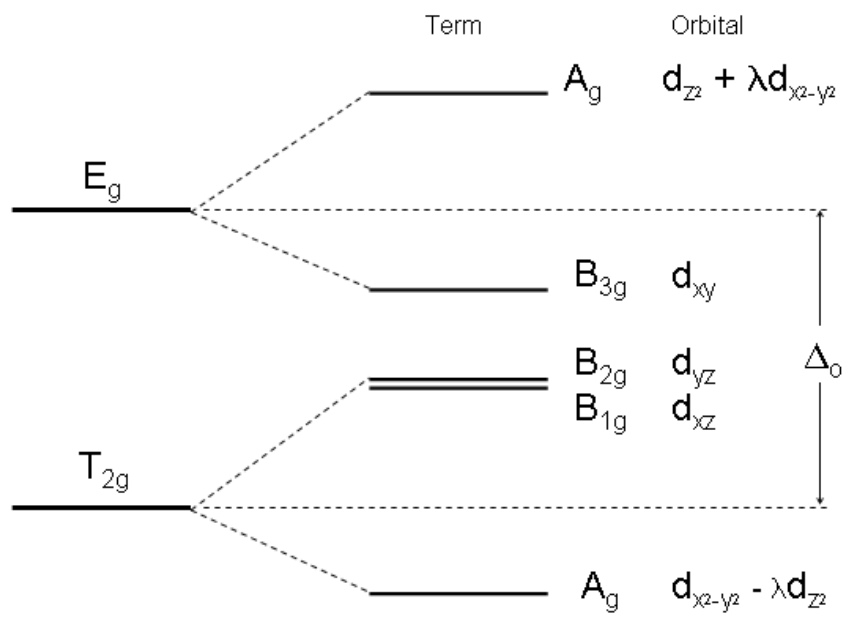
Fig. 4. Energy level diagram for V (IV) in octahedral coordination [21,22].
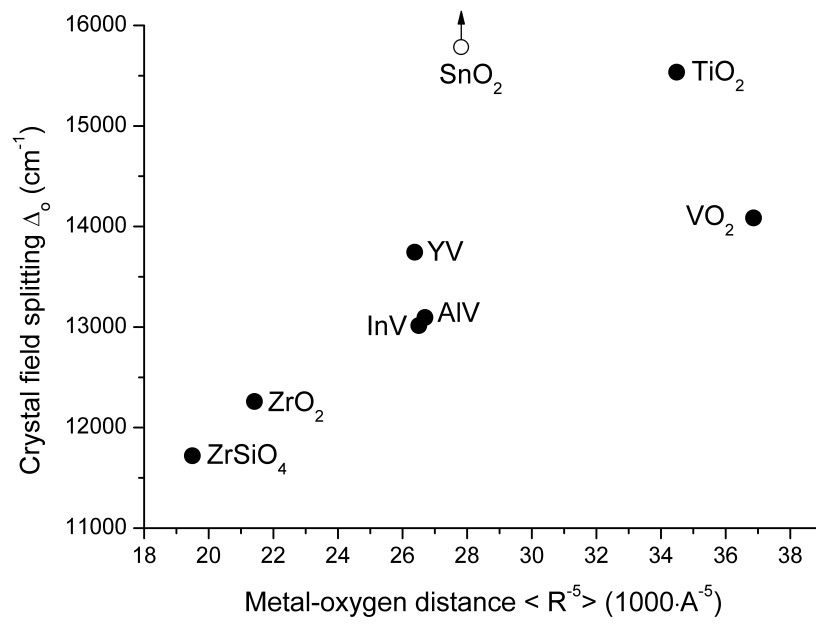
Fig. 5. Crystal field splitting of V^{4+} in octahedral coordination (Δ_o) vs. The inverse fifth power of the mean metal-oxygen distance ($<R^{-5}>$) in zirconium titanate-stannate, several oxides and zirconium silicate.
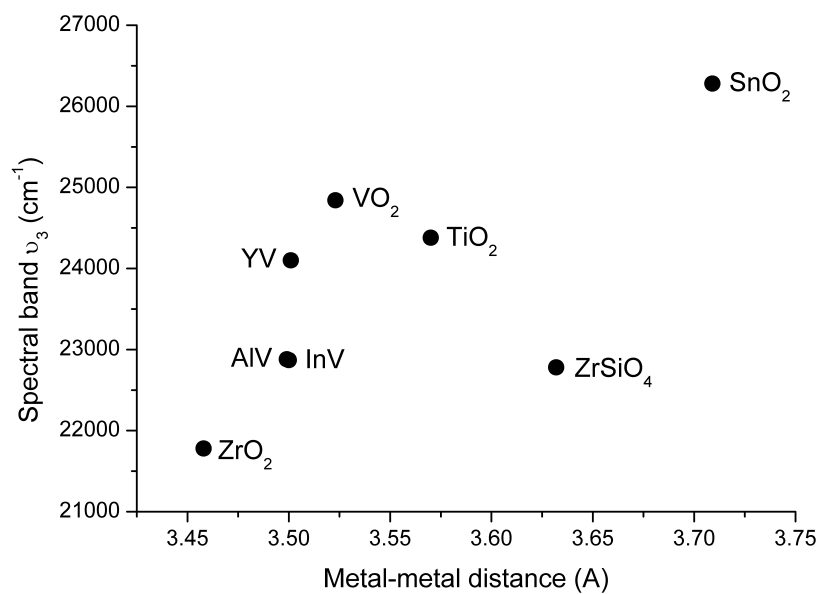
Fig. 6. Positive correlation of the spectral band υ_3 with the metal-metal mean distance between adjacent octahedral sites in zirconium titanate-stannate, several oxides and zirconium silicate.
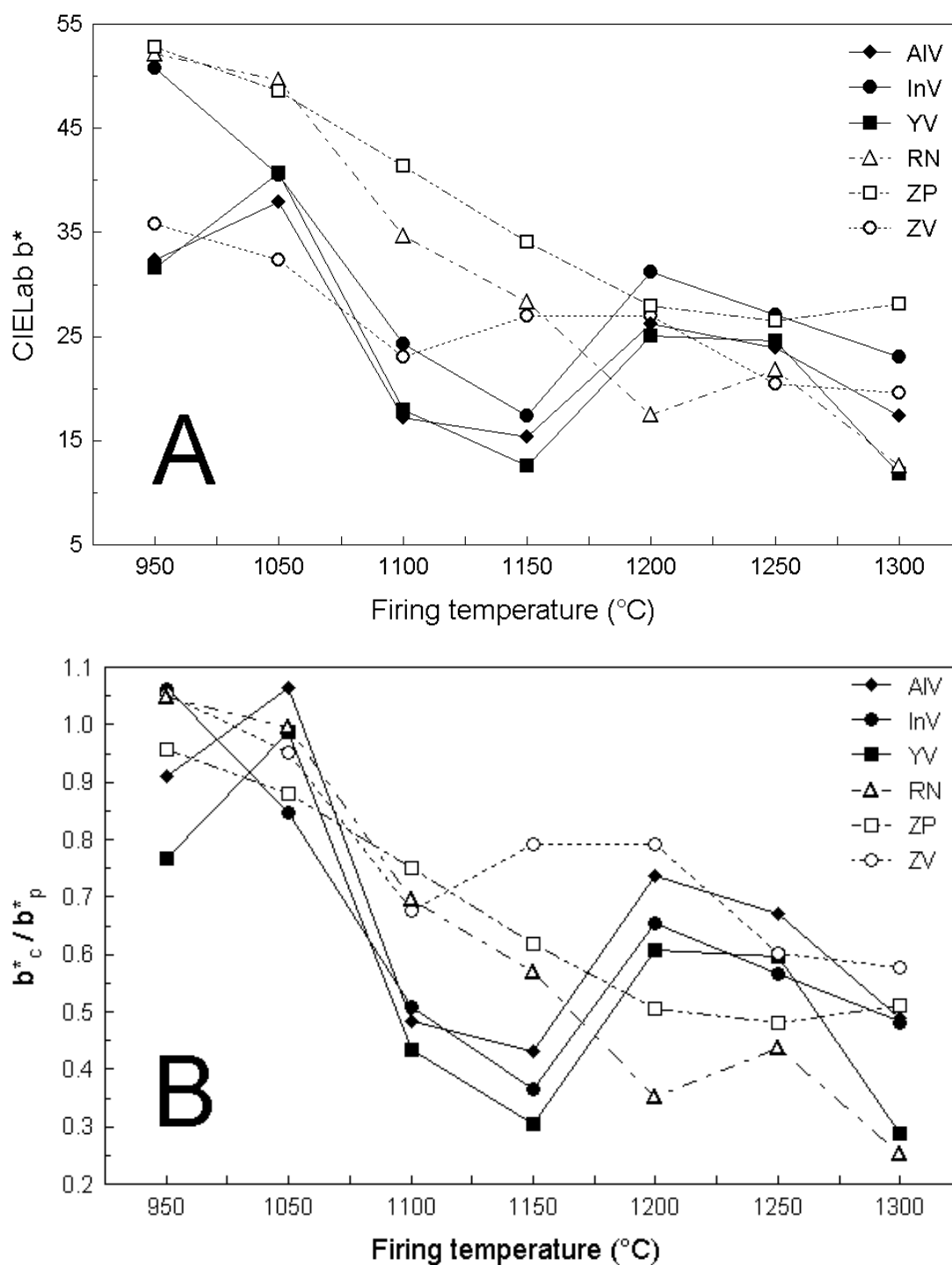
Fig. 7. Colouring performance of zirconium titanate-stannate pigments in different ceramic bodies, glazes and glassy coatings. A) Intensity of yellow shade; B) thermal stability expressed as variation of yellow colour in the ceramic matrix (b^*_g) with respect to the pigment (b^*_p) , i.e. the b^*_g / b^*_p ratio.

Fig. 8. Factorial analysis of technological behaviour of the $ZrTi_{0.47}Sn_{0.47}V_{0.03}In_{0.03}O_4$ pigment in ceramic bodies, glazes and glassy coatings. Extraction of principal components with explained variance: 49.9% (factor 1) and 21.6% (factor 2).

Fig. 9. Colour saturation achieved with the srilankite-type pigment YV in comparison with industrial ceramic pigments.

Table 1

Rietveld figures-of-merit, crystallographic parameters and phase composition of the srilankite-type and industrial ceramic pigments.
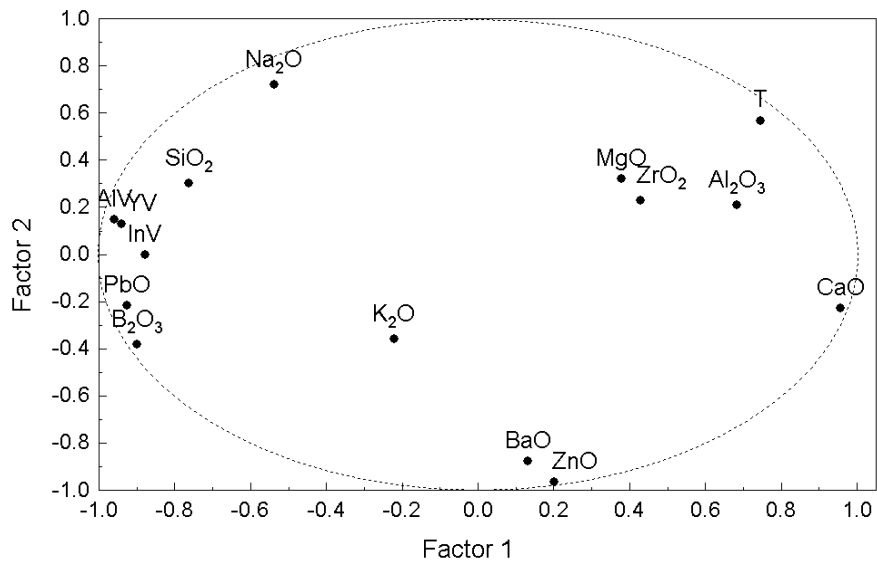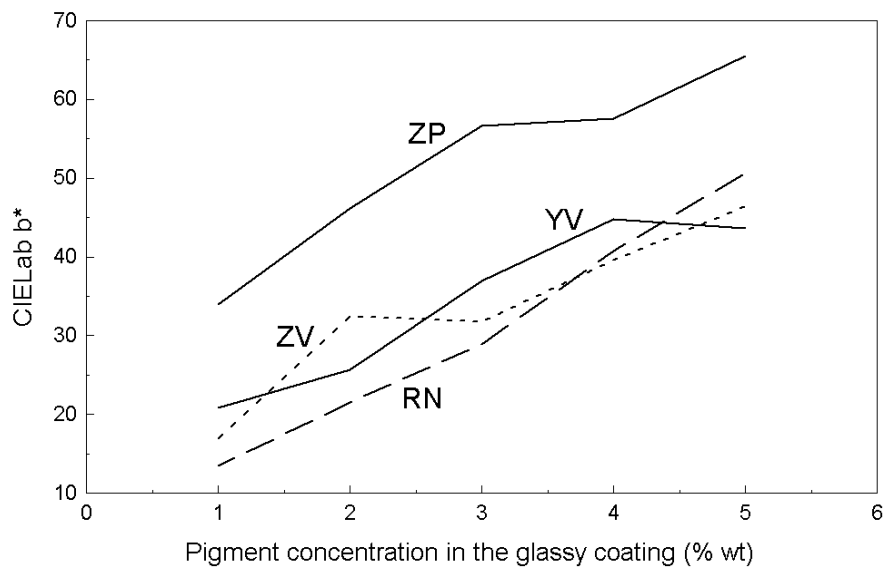
| Parameter | Srilankite-type ceramic pigments | | | | | Industrial ceramic pigments | | |
| | $ZrTi_{0.5}Sn_{0.5}O_4$ [6] | $ZrTi_{0.7}Sn_{0.3}O_4$ [7] | $ZrTi_{0.47}Sn_{0.47}V_{0.03}M_{0.03}O_4$ (this work) | | | $(Ti,Ni,Sb)O_2$ | $(Zr,Pr)SiO_4$ | $(Zr,V)O_2$ |
			M=Al	M=In	M=Y	RN	ZP	ZV
Sample observations	-	-	242	242	242	32	138	473
RF^2	-	-	0.05	0.04	0.05	0.03	0.04	0.03
R_{wp}	-	-	0.14	0.15	0.16	0.11	0.15	0.12
R_p	-	-	0.12	0.12	0.12	0.08	0.11	0.09
Unit-cell dim.								
a (Å)	4.8145(10)	4.824	4.8479(2)	4.8454(3)	4.8495(3)	4.5976(1)	6.6176(3)	5.1449(2)
b (Å)	5.5961(11)	5.553	5.5916(2)	5.6014(4)	5.5961(3)	4.5976(1)	6.6176(3)	5.2082(3)
c (Å)	5.1050(9)	5.083	5.1161(2)	5.1212(3)	5.1201(3)	2.9667(1)	5.9898(2)	5.3149(3)
volume (Å³)	137.54	136.16	138.68	138.99	138.95	62.71	262.31	140.58
Phases (%wt)								
srilankite	100	100	100	100	100	-	-	-
rutile	-	-	-	-	-	88.7(1)	-	-
anatase	-	-	-	-	-	8.8(3)	-	-
zircon	-	-	-	-	-	-	56.7(6)	20.4(4)
baddeleyite	-	-	-	-	-	-	-	60.0(6)
quartz	-	-	-	-	-	2.5(2)	43.3(5)	19.6(5)

Note: Figures in parentheses are standard deviations in the last decimal figure.

Table 2
Atomic positions, metal-oxygen and metal-metal distances of the zirconium titanate-stannate pigments.

Parameter	$ZrTi_{0.5}Sn_{0.5}O_4$	AIV	InV	YV
Atomic positions				
y (Zr,Ti,Sn)	0.1885(2)	0.1885(3)	0.1873(5)	0.1884(3)
x (O)	0.2711(8)	0.272(2)	0.268(2)	0.266(2)
y (O)	0.3988(7)	0.394(2)	0.396(2)	0.397(2)
z (O)	0.4262(9)	0.432(1)	0.424(2)	0.424(2)
Metal-oxygen distances (Å)				
$M-O_{1,2}$ (equatorial)	1.974(3)	1.983(4)	1.961(4)	1.956(4)
$M-O_{3,4}$ (apical)	2.046(3)	2.021(4)	2.065(4)	2.072(5)
$M-O_{5,6}$ (equatorial)	2.157(4)	2.188(4)	2.175(4)	2.178(4)
$<M-O>_{1,2,5,6}$ (equatorial)	2.066	2.086	2.068	2.067
$<M-O>_{1,2,3,4,5,6}$	2.059	2.064	2.067	2.069
Metal-metal distances (Å)				
$M_1-M_{2,3}$	3.312(1)	3.315(1)	3.311(1)	3.317(2)
$M_1-M_{4,5,6,7}$	3.575(1)	3.591(1)	3.594(1)	3.593(1)
Quadratic elongation Δ_6	1.34	1.86	1.79	1.92

Note: Figures in parentheses are standard deviations in the last decimal figure.

Table 3

Optical properties of the zirconium titanate-stannate and industrial yellow ceramic pigments.

Colourimetry	$ZrTi_{0.47}Sn_{0.47}V_{0.03}M_{0.03}O_4$			Industrial pigments		
	M=Al	M=In	M=Y	RN	ZP	ZV
L*	65.7	66.7	75.2	79.5	76.8	66.7
a*	0.0	2.3	-1.8	-3.2	0.1	4.9
b*	35.6	47.8	41.2	49.8	55.8	34.0
Colour purity	47.5	61.1	48.7	55.2	62.8	45.8
Electronic absorptions						
ν_1 peak centre (cm^{-1})	12270	12510	12150	12200	-	11530
FWHM (cm^{-1})	3790	3380	3170	1980	-	3630
Peak fitted area (a.u.)	205	152	99	146	-	207
ν_2 peak centre (cm^{-1})	15580	15670	15540	13730*	-	14270
FWHM (cm^{-1})	3320	3060	3290	1570*	-	940
Peak fitted area (a.u.)	389	246	258	119*	-	26
ν_3 peak centre (cm^{-1})	22880	22870	24100	24480	23140	21780
FWHM (cm^{-1})	7810	5910	7140	5910	5140	5860
Peak fitted area (a.u.)	3050	3617	3491	3803	3450	2044
ν_4 peak centre (cm^{-1})	28210	26090	26430	26390	25950	25760
FWHM (cm^{-1})	8530	4690	3940	2710	3310	5910
Peak fitted area (a.u.)	2031	2298	1141	1113	1943	3516

* further band at 14980 cm^{-1} (FWHM: 1160 cm^{-1}, peak area 53)

Table 44

Optical transitions, crystal field splitting Δ_o, mean metal-oxygen and metal-metal distances and of V^{4+} in several oxides with different coordination and size of the ionic site.

Term	Term	ZrTi$_{0.47}$Sn$_{0.47}$V$_{0.03}$M$_{0.03}$O$_4$			VO$_2$	TiO$_2$	SnO$_2$	ZrO$_2$	ZrSiO$_4$
O_h	D_{2h}	M=Al	M=In	M=Y	rutile	rutile	rutile	baddeleyite	zircon
^2E_g	^2A_g	22880	22870	24100	24840	24380	26280	21780	22780
	$^2B_{3g}$	15580	15670	15540	13900	17750	23230	14270	15560
$^2T_{2g}$	$^2B_{1g}$ $^2B_{2g}$	12270	12510	12150	10570	11060	9100	11530	12360
Coordination		6	6	6	6	6	6	7	8
Δ_o (cm^{-1})		13100	13020	13750	14090	15540	>20000	12300	11720*
<M-O> (pm)		206.4	206.7	206.9	193.5	196.1	205.3	2.157	2.198
<M-M> (pm)		349.9	350.0	350.1	352.3	357.0	370.9	345.8	362.2
Reference	[1921]		[this work]		[1721]			[this work]	

* Crystal field strength expressed as octahedral splitting, i.e. $\Delta_o = 9/8 \Delta_c$